SIRIUS B: A NEW MORE ACCURATE VIEW[2]

J. B. Holberg[1]
Lunar and Planetary Laboratory, Gould-Simpson Bld.,
University of Arizona, Tucson, AZ 85721
Electronic mail: holberg@.argus.lpl.arizona.edu

M. A. Barstow[1]
Department of Physics and Astronomy, University of Leicester,
University Road, Leicester LE1 7RH, United Kingdom
Electronic mail: mab@star.le.ac.uk

F. C. Bruhweiler[1]
Department of Physics, Catholic University of America, Washington D.C., 20064
Electronic mail: hrs::hrsfred

A. M. Cruise
School of Physics and Space Research, University of Birmingham, Edgbaston,
Birmingham, United Kingdom
Electronic mail: amc@star.bham.ac.uk

A. J. Penny
Astrophysics Division, Rutherford Appleton Laboratory,
Didcot, Oxfordshire, OX11 OQX, United Kingdom
Electronic mail: alan.penny@rl.ac.uk

Appeared in the *Astophysical Journal*, 497, 935 (1998)

[1]Guest Observer, *Extreme Ultraviolet Explorer* satellite

[2]Based on observations carried out with the *Extreme Ultraviolet Explorer* satellite, and the ESA *Hipparcos* astrometry satellite and with data obtained from the *IUE* final archives.

ABSTRACT

Long standing questions regarding the temperature, gravity, mass and radius of the well-known white dwarf Sirius B are considered in light of new data. Recently obtained *Extreme Ultraviolet Explorer (EUVE)* observations and reprocessed *IUE* NEWSIPS data have produced a new, well-defined effective temperature of 24,790 $\pm$ 100 K and a surface gravity of log g = 8.57 $\pm$ 0.06 for Sirius B. A new *Hipparcos* parallax for the Sirius system of $\pi = 0.37921'' \pm 0.00158''$ is used in conjunction with the above spectroscopic results and the previously published gravitational redshift to yield a mass of 0.984 $\pm$ $0.074 M_{\odot}$ and a radius of R = 0.0084 $\pm$ $0.00025 R_{\odot}$ for the white dwarf. Combining these results with the existing astrometric mass for Sirius B gives a refined mass estimate of M = 1.034 $\pm$ $0.026 M_{\odot}$. The mass and radius for Sirius B are found to be consistent with the theoretical mass-radius relation for a carbon-core white dwarf. The *EUVE* spectrum is also used to determine a firm upper limit of He/H = 1.8x10^{-5} for the helium mixing ratio in the photosphere of Sirius B. *IUE* echelle spectra of Sirius B provide an estimate of log(N_{HI}) = 17.72 $\pm$ 0.1 for the interstellar H I column to this star.

Subject headings: stars:– atmospheres – stars; individual (Sirius B) – ultraviolet: stars – white dwarfs

1. INTRODUCTION

Although Sirius B is the nearest and brightest of the white dwarfs, it remains an enigmatic object, with intriguing questions concerning its high mass and speculation regarding its origin. In contrast to many other white dwarfs, where the fundamental parameters of temperature, radius and mass can now be estimated with considerable precision, in Sirius B these quantities have remained highly uncertain. This is largely due to the extreme difficulty of observing the much fainter white dwarf in close proximity to the brightest star in the sky, Sirius A. It has long been evident from astrometric measurements (Gatewood & Gatewood 1978) that Sirius B, at 1.05 $M_{\odot}$, is among the most massive white dwarfs known. The general population of hot white dwarfs have masses which are narrowly distributed about a mean of 0.58 $M_{\odot}$. The number of such stars with a mass in excess of 1.0 $M_{\odot}$ is estimated to be less than 2 % of the general population. The large mass of Sirius B therefore offers a unique opportunity to test white dwarf theoretical mass-radius relationships near the limiting Chandresakar mass. This large mass also highlights other intriguing aspects of Sirius B, such as its prior evolution. For example, Sirius B has been implicated in the controversy regarding ancient historical references to the 'reddish' color of Sirius (Schlosser & Bergmann 1985 and Bruhweiler, Kondo & Sion 1986), where Sirius B was suggested to have been a red giant or to have undergone a thermonuclear runaway in historical times. As we shall show, the radius of Sirius B conforms closely to the expected radius for a normal thermally evolved degenerate star, thus providing a strong argument against such scenarios.

The very small angular separation between Sirius B and Sirius A makes Sirius B an extremely challenging object to study in detail. One example of this difficulty is the wide range of effective temperature estimates for Sirius B. Using detailed fits to the H I Balmer lines, it is now common to measure effective temperatures of DA white dwarfs in the temperature range from 20,000 K to 30,000 K to an accuracy of 1 % or better (Bergeron, Saffer, & Liebert 1992). In contrast, modern estimates of the effective temperature of Sirius B have ranged from 22,000 K to 32,000 K (Koester 1979 and Greenstein, Oke & Shipman 1971, respectively). More recent analyses (Holberg, Wesemael, & Hubeny 1984, Paerels et al. 1988 and Kidder, Holberg, & Wesemael 1989) have narrowed this range to 26,000, ± 2000 K. However, the effective temperature (T_{eff}) continues to dominate other sources of uncertainty in the estimation of the stellar radius. For example, at 26,000 K, the ± 7% temperature uncertainty translates into a ± 7% uncertainty in the radius. When combined with additional sources of uncertainty in the visual magnitude and distance, Sirius B appears to lie some distance above the predicted mass-radius relation for carbon-core white dwarfs. Thejll & Shipman (1986), for example, conclude that Sirius B lies $\sim 2\sigma$ above the mass-radius relation and suggest that a high rotational velocity may be necessary to explain the larger than predicted radius. New, accurate estimates of the effective temperature derived from the extreme UV spectra of Sirius B, which is free from contamination by Sirius A, substantially reduce the existing temperature uncertainty and consequently the radius uncertainty.

An accurate effective temperature is a critical step in improving the mass and radius estimates for Sirius B and in turn deciding whether or not this star is consistent with the theoretical mass-radius relation for carbon-core white dwarfs or whether the star is in some way anomalous. As pointed out by Schmidt (1996), the very high mass of Sirius B makes such a comparison especially significant, since it is one of the few truly high-mass white dwarfs for which we have both a good distance estimate and a dynamic mass estimate. Such a comparison takes on added importance in light of the recent demonstration by Shipman et al. (1997) that another well-studied white dwarf with a known astrometric mass, 40 Eri B, can be used to observationaly define the low-mass (0.5 $M_\odot$) end of the white dwarf mass-radius relation. Most other stars, where mass-radius relations can be tested to a similar accuracy, cluster near 0.6 to 0.7 $M_\odot$ and, consequently, reveal little about the overall shape of the mass-radius relation. A solid empirical confirmation of the overall white dwarf mass-radius relationship is important not only because such relationships are now routinely used to estimate white dwarf masses and radii, but also because the models they are based on play an important role in such diverse areas as estimating the distance to globular clusters (Renzini et al. 1996) and the age of the galactic disk (Wood 1992).

In this paper we combine both new and archive spacecraft observations of Sirius B to significantly improve estimates of its effective temperature, surface gravity, mass and radius. In §2.1, a recent high quality *Extreme Ultraviolet Explorer (EUVE)* spectrum of Sirius B is analyzed to yield a dramatically improved estimate of its effective temperature and to place new spectroscopic limits on the presence of helium in the stellar photosphere. In §2.2, archive *IUE* low dispersion spectra are coadded to produce a Lyman α profile from which an improved estimate of the Sirius B surface gravity is obtained. High dispersion *IUE* spectra are used to help constrain the interstellar H and He columns along the line of sight to Sirius B, which, among other things, are critical in the modeling of the *EUVE* spectrum. Finally, in §2.3, we employ the newly available *Hipparcos* parallax for Sirius B to improve its radius estimate. In §3.3, these parameters are used to calculate mass and radius estimates for Sirius B which are compared with the existing astrometric mass of Sirius B and with theoretical mass-radius relations.

2. OBSERVATIONS

2.1. *EUVE* OBSERVATIONS

EUVE Guest Observer (GO) observations of Sirius B were conducted between 27 November and 2 December 1996. A total integration time of 92,450 sec. was achieved. These observations were performed in the 'dithered' mode in which the stellar image is moved in a spiral pattern over the detector in order to reduce instrumental fixed pattern noise. Barstow, Holberg, & Koester (1995), have demonstrated that dithering can result in as much as a 4:1 improvement in spectral signal-to-noise ratio (S/N). Useful stellar signal was only obtained in the short wavelength (SW) 70 Å to 190 Å and medium wavelength (MW) 140 Å to 350 Å spectrometers. Extracted one-dimensional spectra were produced from standard *EUVE* GO processed event data using IRAF procedures. A 20 pixel-wide extraction aperture was used and the subtracted background spectrum was retained for the computation of count rate statistics. A combined SW and MW extracted spectrum, covering the 80 Å to 270 Å wavelength range, of Sirius B is shown in Fig. 1. The *EUVE* spectrum of Sirius B was modeled using an extensive set of grids of homogeneous and stratified H/He model atmospheres computed by D. Koester (see Koester 1991). Fits of these models to the data were done using the spectral fitting program XSPEC (Schafer et al. 1991) and employed procedures similar to those used in Barstow et al. (1994a,b). The interstellar absorption model contains the H I, He I and He II continua described in Rumph, Bowyer, & Vennes (1994).

Taken alone, the *EUVE* data can be successfully fit using several combinations of stellar and interstellar parameters. A fundamental difficulty in obtaining a unique result is the lack of accurate knowledge concerning the interstellar column to Sirius B. Because the column is apparently well below $N_{HI} = 10^{18}$ cm^{-2}, no obvious features due to interstellar He I and He II are seen; yet continuum absorption from these ions is certainly present. In §3 we discuss the use of external information to constrain the ISM column to Sirius B.

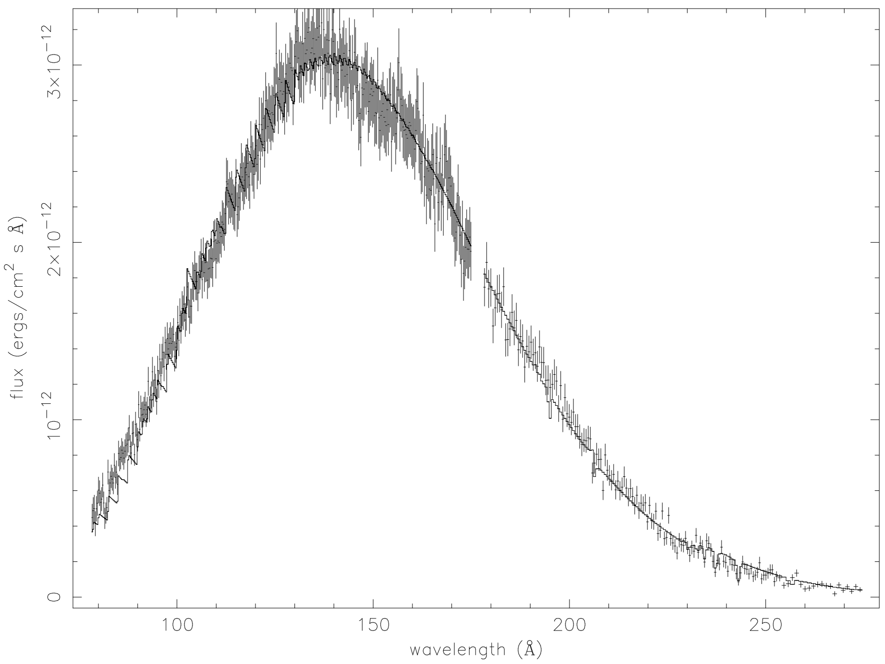

Fig. 1.— *EUVE* spectrum of Sirius B showing combined SW and MW spectra. The model shown as a fit to these data incorporates a stellar continuum and absorption from interstellar H and He as discussed in the text. The sawtooth features in the model shortward of the flux peak are numerical artifacts of the instrumental deconvolution.

2.2. *IUE* OBSERVATIONS

In Table 1 we list eight *IUE* spectra of Sirius B which were obtained from the *IUE* Data Analysis Center. These data are mostly NEWSIPS (NASA *IUE* Newsletter 53) images of three distinct types. First, is the large-aperture, low-dispersion image SWP 02751, which was initially analyzed by Böhm-Vitense, Dettmann & Kapranidis (1979, hereafter BDK). In this observation, Sirius B, which at the time, had an apparent distance of $10.8''$ from Sirius A, was placed near one end of the $10''$ by $20''$ large-aperture slit, so as to minimize the scattered light from Sirius A. In §2.2.1 we reanalyze the NEWSIPS version of this image in an attempt to obtain an improved determination of Lyman α profile and the absolute UV flux from Sirius B. This absolute flux distribution is combined with the second set of *IUE* data, consisting of three small-aperture, low-dispersion, NEWSIPS images of Sirius B, to obtain a coadded SWP spectrum on an absolute scale. These three images (SWP 10076, SWP 10122 and SWP 10123) were obtained by Savedoff in 1980 when the separation of components A and B was still $10.2''$. The third set of images consists of high dispersion spectra of Sirius B also obtained through the large and small apertures. SWP 02750 is a large-aperture echelle image obtained by BDK at the same orientation as SWP 02751 and is contaminated by Sirius A longward of 1300 Å. The small-aperture image SWP 10075 was obtained by Savedoff and discussed in Bruhweiler & Kondo (1982), while the remaining two (SWP

22693 and SWP 22694) were obtained by Gry in 1984 when the A-B separation was 8.6″. We have not attempted to coadd these spectra since SWP 22693 and SWP 22694 are not yet available in NEWSIPS format. Weak interstellar lines due to Si II, C II, and O I are found in these spectra and are used in a following section to estimate the H I column to the Sirius system.

Table 1: *IUE* Images of Sirius B

IUE Image	Ap./Disp.	Date	Dur(s)	Exp.	Observer
SWP 02750	L/H	28 Sep. 1978	1000	255/15	Böhm-Vitense
SWP 02751	L/L	28 Sep. 1978	9.7	220/15	Böhm-Vitense
SWP 10075	S/H	10 Sep. 1980	1200	189/41	Savedoff
SWP 10076	S/L	10 Sep. 1980	23.6	218/17	Savedoff
SWP 10122	S/L	14 Sep. 1980	23.6	218/17	Savedoff
SWP 10123	S/L	14 Sep. 1980	23.6	218/17	Savedoff
SWP 22693	S/H	08 Apr. 1984	1200	401	Gry
SWP 22694	S/H	08 Apr. 1984	1200	401	Gry

2.2.1. ANALYSIS OF IUE *IMAGE SWP 02751*

An analysis of the large-aperture image SWP 02751, obtained on 28 September 1978, was originally presented by BDK. Here we re-analyze this image, obtained from the *IUE* Archives, using NEWSIPS processing, in order to obtain an improved extraction of the Sirius B spectrum on an absolute scale. NEWSIPS reprocessing offers a number of opportunities to improve upon the original analysis of BDK. NEWSIPS improvements include, among other things, an enhanced Intensity Transfer Function (ITF), corrections for the sensitivity degradation of the instrument, a more accurate sampling of the image, and a new absolute calibration. In addition to these general enhancements, the resampled and geometrically corrected data allow a substantially better assessment of light loss due to both the edge of the slit and subtraction of the scattered light from Sirius A in SWP 02751.

A customized extraction of the Sirius B spectrum from the resampled, photometrically corrected version ('SILO' file) of SWP 02751 was performed in the following manner. A region consisting of two strips (lines 32 to 38 and 64 to 70), external to the large-aperture, was subtracted to remove detector background counts. The dispersed Sirius B image was found to peak in the cross-dispersion direction at line 45 (see Fig. 2). In comparison, the nominal slit center is line 51 and the slit edge is located at line 43. In angular units, Sirius B is determined to be displaced from the center by $9.0'' \pm 0.2''$ along the long axis of the slit. Since the total slit width is officially determined to be $21.65'' \pm 0.39''$ (NASA *IUE* Newsletter 53), this indicates the star was located approximately 1.8″ from the edge of the slit. At this position, light from Sirius B suffers a modest amount of attenuation.

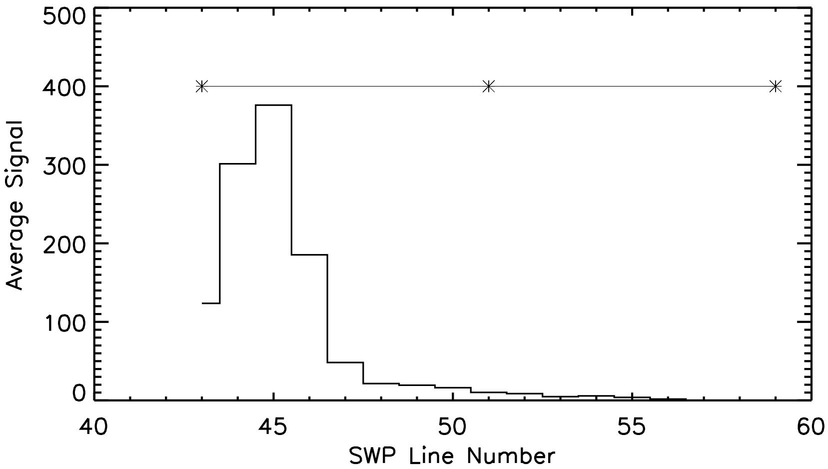

Fig. 2.— A cross-dispersion plot of *IUE* image SWP 02751 in the 1250 Å to 1350 Å region. The approximate center and length of the SWP large-aperture are indicated by the asterisks and line above the plot. The scattered light component from Sirius A is evident as a broad tail extending to the right.

In order to estimate the extent of this attenuation, trailed low-dispersion images of two white dwarfs (G191-B2B, SWP 15728 and 40 Eri B, SWP 07973) were used to define a normalized photometric response of the SWP Large-Aperture slit, including the edges. From this slit response image it is evident that the transmission, at the location of Sirius B, is somewhat wavelength dependent, decreasing monotonically from 1.0 in the 1250 to 1350 Å region to 0.70 in the 1850 to 1950 Å region. The normalized slit response image was divided into the slit image of SWP 02751.

Next it was verified that the scattered light from Sirius A had the expected spectral character of an A0 V star by comparing it with an extracted spectrum of δ UMa (SWP 10118). This scattered light component was removed by modeling it as a simple linear gradient in the cross-dispersion direction and as an A0 V stellar spectrum in the dispersion direction. This is essentially the same scattered light model used by BDK. A cross-dispersion cut through SWP 02751, between wavelengths 1250 Å to 1350 Å is shown in Fig. 2. In order to avoid large attenuation corrections near the slit edge, an asymmetric spectral extraction was performed using lines 45 through 47. A similar asymmetric extraction was applied to the spectrum of the DA white dwarf CD -38° 10980 in SWP 20340 to assess any photometric biases.

The final extracted spectrum of Sirius B was compared with a model atmosphere. The uncertainty in the absolute flux level in the vicinity of 1250 Å in Fig. 3 was estimated to be $\pm$ 5%, although, as discussed in §3.2, the V magnitude which corresponds to this flux level appears to be too high, indicating that the true uncertainty of the absolute flux scale is nearer 10 %. The absolute flux level is used to normalize the three small-aperture spectra of Sirius B which were then coadded with the extracted SWP 02751 spectrum. This effectively places the resulting coadded Sirius B spectrum on the *IUE* NEWSIPS flux scale. Kidder et al. (1988) had previously demonstrated that the small-aperture spectra in Table 1 were free of contamination from Sirius A.

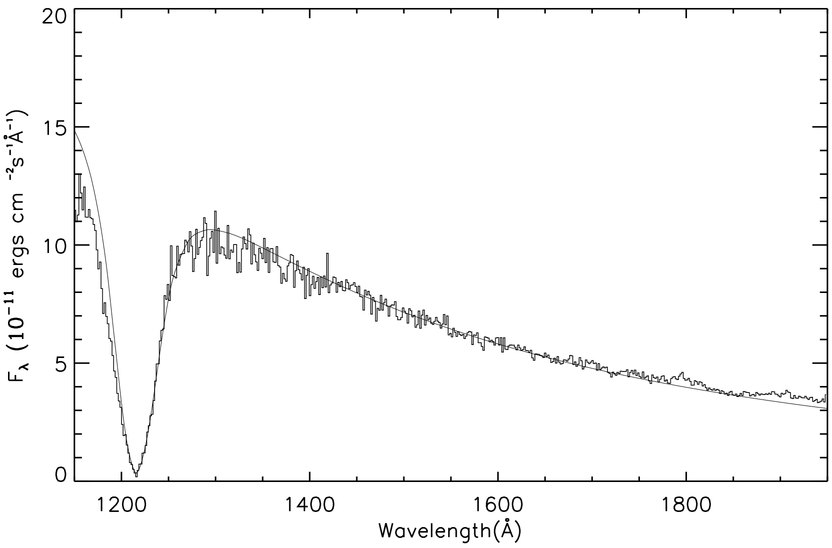

Fig. 3.— A coadded SWP spectrum of Sirius B scaled to the flux in SWP 02751. The three small aperture, low-dispersion images in Table 1 have been combined with SWP 02751. The continuous curve is a 24,800 K, log g = 8.61 model atmosphere scaled to V = 9.0

2.2.2. IUE *Echelle Spectra*

Previous determinations of the neutral hydrogen column density, N_{HI}, to the Sirius system have relied upon indirect estimates based on observations of interstellar species other than H I. BK82 analyzed the echelle image SWP 10075 and found weak features due to Si II λ1260, O I λ1302, and C II λ1334. The authors used these to estimate an H I column density of log(N_{HI}) = 17.93 to Sirius B. We have reexamined SWP 10075 and the three additional echelle images of Sirius B in Table 1; two of these are in NEWSIPS format (SWP 10075 and SWP 02750) and two are in IUESIPS format (SWP 22393 and SWP 22394). In each of the four spectra, we confirm the existence of the three ISM features found by BK82 but are unable to find any additional lines. Equivalent widths of 47 $\pm$ 6 mÅ , 74 $\pm$ 14 mÅ and 97.5 $\pm$ 14.7 mÅ for Si II, O I and C II, respectively were obtained. Corresponding upper limits for the Si II $\lambda\lambda$ 1304 and 1526 ISM lines are estimated to be 25 mÅ.

To estimate column densities for these species, BK82 assumed a Doppler parameter of $b = 15$ km s^{-1}. The present state of knowledge concerning the line of sight to the Sirius system is much improved compared to that assumed by BK82. For example, Lallement et al. (1994), using Hubble Space Telescope (HST) high dispersion observations of Mg II and Fe II, find the line-of-sight to

Sirius A to consist of two Doppler components, a dominant component at +19.5 km s^{-1} and a less prominent component at +13.7 km s^{-1}. Moreover, they find both components to be relatively warm ($\sim$ 7000 K) with low Doppler parameters of $\sim$3 km s^{-1}. Although *IUE* cannot resolve these components, it is possible to use this information to improve *IUE* column density estimates. We adopt a simplified model of the Sirius B line-of-sight based on the results of Lallement et al. by assuming the two clouds are sufficiently separated in velocity that they have independent curves of growth and that they differ significantly only in their total column densities which are in a ratio of 1:1.7. If both have a characteristic kinetic temperature of 7600 K, and turbulent velocities of ξ =1.4 km s^{-1}, then mass-dependent Doppler parameters of 2.5 km s^{-1}, 3.1 km s^{-1}, and 3.5 km s^{-1} are obtained for Si II, O I, and C II, respectively. From our equivalent widths, the corresponding column densities are, $\log(N_{SiII}) = 12.88 \pm 0.13$, $\log(N_{OI}) = 14.49 \pm 0.27$, and $\log(N_{CII}) = 14.34 \pm 0.30$. These can be used to estimate H I column densities from the solar abundances for each species and its depletion in the LISM. Using solar abundances from Savage & Sembach (1996) and logarithmic depletion factors characteristic of the warm ISM of -0.43 for Si and 0.0 for O and C, we obtain estimates of $\log(N_{HI})$ = 17.76, 17.36 and 17.56, respectively and a weighted mean value of 17.72 $\pm$ 0.1. These values are approximately 0.2 dex lower than that obtained by BK82. The difference is primarily due to splitting the absorption between the two clouds, and our use of a lower Doppler parameter. Our estimate of $\log(N_{HI}) = 17.72 \pm 0.1$ is somewhat larger than that of Bertin et al. (1995) who found $\log(N_{HI}) = 17.53^{+0.11}_{-0.15}$ from the ISM deuterium column density to Sirius A and an assumed D/H ratio for the LISM. Our value is also somewhat less than that of Frisch (1994) who obtained 17.89 from the Lallement et al. Mg II column density to Sirius B.

2.3. *Hipparcos* OBSERVATIONS

A new absolute trigonometric parallax for the Sirius system was obtained from the final results of the *Hipparcos* mission (ESA 1997). These observations were obtained under a 1992 proposal to the 'Hipparcos Research Programme', within mission consortia, to determine the distances to a selected set of white dwarfs detected as ROSAT EUV sources. *Hipparcos* parallaxes represent an unprecedented improvement in both the number and quality of trigonometric parallax measurements. For example, Arenou et al. (1995) have shown *Hipparcos* parallaxes have a zero point accurate to better than 0.5 milliarcsec and have external errors are which correctly estimated to within 5 %. The Sirius B parallax, $\pi = 0.37921'' \pm 0.00158''$, is consistent with, but represents a 20 % reduction in the uncertainty over, the ground based parallax of $\pi = 0.3803'' \pm 0.0020''$ given in van Altena et al. (1991). The new *Hipparcos* distance to the Sirius system corresponds to a distance of 2.637 $\pm$ 0.011 pc. In §3.3 we use this new parallax in conjunction with photometric and spectroscopic data to determine a consistent estimate of the mass and radius of Sirius B which can be compared with theoretical mass-radius relationships.

3. ANALYSIS AND DISCUSSION

3.1. Analysis of the *EUVE* Spectrum of Sirius B

As discussed in the introduction, lack of accurate values for the effective temperature and gravity of Sirius B have hampered efforts to compare it with theoretical mass-radius relationships. Were Sirius B not so seriously contaminated by scattered light from Sirius A, it would not be simple to obtain accurate values of these quantities from fits to the Balmer line profiles. Because accurate observations of the Balmer lines are not practical during the current epoch of small angular separations, we use the temperature-sensitive *EUVE* spectrum together with the *IUE* Lyman α profile to constrain both the effective temperature and surface gravity of Sirius B.

The *EUVE* spectrum is quite sensitive to T_{eff} but less so to log g. In the case of Sirius B, an accurate *EUVE* determination of T_{eff}, however, also depends on independent knowledge of the ISM column to the star. For example, models with T_{eff} = 25,400 K, log (N_{HI}) = 18.85, and T_{eff} = 25,160 K, N_{HI} = 0 both can be made to fit the data. This correlation between T_{eff} and ISM column can be further influenced by the He I and He II contributions to the ISM absorption. Unlike stars with larger ISM columns (Barstow et al. 1997a), none of these ISM parameters can be uniquely determined from the Sirius B *EUVE* data alone. In order to constrain the *EUVE* fits, we use our *IUE* echelle results (see §2.2.2) for the total H I column to Sirius B of log (N_{HI}) = 17.72 ± 0.1. Further, we assume a value of the cosmic H to He ratio of 10 and the ISM He ionization ratio (He II to total He) of 0.27 ± 0.04 (Barstow et al. 1997a). The latter assumption is based on the detailed analysis of *EUVE* results for a number of nearby white dwarfs (Barstow et al. 1997a) and are supported by recent estimates of the electron density (Wood & Linsky 1997) and He and H densities (Gloeckler, Fisk, & Geiss 1997) within the local cloud. The resulting He I and He II column densities are log (N_{HeI}) = 16.77 and log (N_{HeII}) = 16.34. These results are consistent with the 3 σ upper limits of $\log(N_{HeI}) = 16.92$ and $\log(N_{HeII}) = 16.82$, which can be inferred from the lack of observed spectral features due to He I and He II features in the Sirius B spectrum.

Having constrained the ISM absorption, we next analyze the *EUVE* spectrum in terms of its effective temperature, composition and surface gravity. In this analysis, we employ both homogeneous and stratified models as well as models having an arbitrarily low He content. We also model the combined *EUVE* and *IUE* Lyman α data sets (see §3.2). Results of these analyses are shown in Table 2. One model is of particular interest. In Fig. 4 we show the 180 Å to 270 Å region and the homogeneous model fit containing a He/H abundance ratio of 1.8x10^{-5}. This He abundance is primarily a consequence of the overall shape of the *EUVE* spectrum. Evident near the He II Lyman edge at 228 Å, however, are possible counterparts to photospheric lines at 243 Å and 237 Å, which are the He II Lyman δ and λ lines, respectively. If real, these lines would represent the first spectral detection of He II in Sirius B. Significantly, Paerels et al. (1988), in their analysis of the Sirius B *EXOSAT* transmission grating spectrum, also find evidence for the presence of He/H = 10^{-5} at the 3 σ level in Sirius B. However, spectral features due to He were not evident in that much lower-resolution spectrum.

Table 2: Fits to the *EUVE* and *IUE* Spectra

Data	Model	Parameters and χ^2/ν
EUVE	homogeneous	T_{eff} = 25,000 ± 35 K
		$\log g$ = 8.51 ± 0.03
		He/H = 4.8 ± 1.1 x10^{-6}
		χ^2/ν = 1.17
EUVE	stratified	T_{eff} = 24,600 ± 50 K
		$\log g$ = 8.50 ± 0.03
		H_{layer}= 1.13 ± 0.01 x10^{-13}
		χ^2/ν = 1.17
EUVE + Ly α	He = 10^{-8}	T_{eff} = 24,496 ± 100 K
		$\log g$ = 8.68 ± 0.05
		χ^2/ν = 1.57
EUVE + Ly α	homogeneous	T_{eff} = 24,790 ± 100
		$\log g$ = 8.57 ± 0.06
		He/H = 4.0 ± 1.0 x10^{-6}
		χ^2/ν = 1.44

Fixed values:
EUVE: $\log(N_{HI})$ = 17.92, $\log(N_{HeI})$ = 16.92, $\log(N_{HeII})$ = 16.82
EUVE + Ly α: V = 8.44, $\log(N_{HI})$ = 17.72, $\log(N_{HeI})$ = 16.77, $\log(N_{HeII})$ = 16.34

The presence of trace levels of He in DA white dwarfs is of considerable importance for several reasons. First, it is the presence or absence of He which defines the two primary spectroscopic classes of white dwarf, the H-rich DA stars and the He-rich DB and DO stars (Sion et al. 1983). The evolutionary circumstances leading to these two types remains unclear as does the question of whether or not the two classes of white dwarf can metamorphose into one another as they cool. The latter interpretation receives some support from observed changes with temperature in the ratio of the number of He-rich to H-rich white dwarfs. Second, theoretical considerations of diffusion time scales for He in DA atmospheres clearly indicate that virtually no He is to be expected at photospheric levels. For example, for stars having masses above 0.8 $M_{\odot}$, He abundances should be less than 10^{-8}. The detection of trace levels of He could, in principle, shed light on these issues. Unfortunately, as in the case of HZ 43 (Barstow et al. 1995), the present *EUVE* data can only hint at the presence of He. An *F*-test of the data in this region indicates that these lines cannot be regarded as statistically significant. We will adopt this conservative interpretation and treat the He abundance as an upper limit.

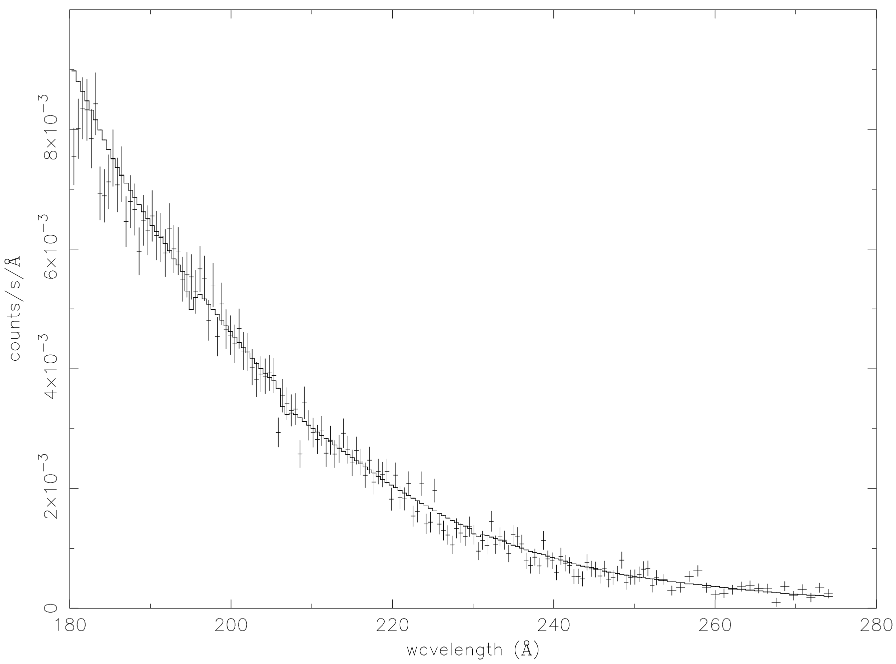

Fig. 4.— The 200 Å to 270 Å region of the *EUVE* spectrum of Sirius B containing the He II Lyman series limit at 228 Å. The possible features at the location of the Lyman ϵ and δ lines are used to place an upper limit to the helium content in the photosphere of Sirius B. The model is discussed in the text.

Adopting a homogeneous model with the above He abundance and the previously discussed ISM column we find T_{eff} = 25,000 ± 35 K (internal statistical uncertainty) and log g = 8.51 ± 0.04. This result is consistent with the values obtained by Paerels et al. (1988) of T_{eff} = 25,500 ± 500 K and log g = 8.63 ± 0.1, from their analysis of the *EXOSAT* grating spectrum of Sirius B.

3.2. Analysis of the *IUE* Spectrum of Sirius B

A fit of the Sirius B Lyman α profile alone yields T_{eff} = 24,360 ± 285 K and log g = 8.61 ± 0.15. This temperature is very similar to that of Kidder et al. (1988) who also fit a small aperture SWP Lyman α profile to get T_{eff} = 24,500 ± 500 K. We can improve our results by constraining the temperature to be consistent with the more sensitive *EUVE* result (see Table 2). When this is done, we find T_{eff} = 24,790 ± 100 K and log g = 8.57 ± 0.06. Using this temperature, it is possible to estimate the visual magnitude of Sirius B from the absolute flux of the coadded SWP spectrum in Fig. 3. From the model atmosphere and theoretical V magnitude normalization of Bergeron, Wesemael, & Beauchamp (1995), we estimate V = 8.56 ± 0.05. This is at the faint end of the range of published V magnitudes for Sirius B and indicates that the absolute UV flux of Sirius B in Fig. 3 may be underestimated. Another indication of this difficulty is the fact that, to jointly fit the *EUVE* and *IUE* data sets, it was necessary to allow the fitting software to adjust the scaling of the *IUE* data.

Several measurements of the visual magnitude of Sirius B have been published including V = 8.29 ± 0.10 (Hardie, 1969), V = 8.37 ± 0.05 (Lindenblad, 1970) and V = 8.44 ± 0.03 (Rakos & Havlen 1977). Of these, the photoelectric results of Rakos & Havlen are judged the most reliable since their observed Johnson and Stromgren colors are reasonable matches to the predicted colors of Bergeron et al. (1995) for a 24,800 K white dwarf. However, from the Rakos & Havlen colors it is also evident that they have underestimated their uncertainties. We adopt the value V = 8.44 ± 0.06.

3.3. Mass and Radius of Sirius B

In order to estimate the mass and radius of a white dwarf as well as other fundamental parameters, such as its luminosity or age, one frequently adopts a theoretical mass-radius relationship. In the past, this choice was most often made from zero-temperature (fully degenerate) mass-radius relationships such as those of Hamada & Salpeter (1961). Currently, more realistic models (Wood 1995) are used, which follow the thermal evolution of white dwarfs as they cool and which also account for several different possible configurations of hydrogen and/or helium in the outer layers; it is most common to assume a carbon core. In general, thermal effects are most pronounced in hot ($T_{eff} > 30{,}000$ K) and low-mass (M < 0.55 $M_{\odot}$) white dwarfs. At lower temperatures and higher mass, evolutionary models closely resemble zero-temperature models.

Sirius B provides a unique opportunity to compare observations with theoretical mass and radius predictions for a 1 $M_{\odot}$ white dwarf. The analytical approach which we adopt is similar to that discussed in Barstow et al. (1997b) for V 471 Tau except that we have, as an additional condition, a measured gravitational redshift for Sirius B (Greenstein et al., 1971). In all, we possess high precision measurements of the trigonometric parallax from *Hipparcos*, as well as spectroscopic determinations of surface gravity and gravitational redshifts. From each of these pieces of information, together with T_{eff} and the V magnitude (see Table 3), it is possible to independently estimate a stellar radius. From the parallax one can use the spectroscopically determined effective temperature and absolute flux, (most often the V magnitude) to calculate a stellar radius using the fundamental equation:

$$F_{\lambda} = 4\pi(\frac{R_{\pi}^2}{D^2})H_{\lambda}(T, \log g), \qquad (1)$$

which relates the observed monochromatic flux F_{λ} to the Eddington flux $H_{\lambda}(T, \log g)$ at the stellar surface through the stellar solid angle (R^2/D^2). Here R is the stellar radius and D is the distance given by the parallax π. The Eddington flux can be specified with considerable confidence and accuracy using emergent fluxes calculated from model atmospheres. We use the results of Bergeron, Wesemael, & Beauchamp (1995) to estimate Eddington fluxes, primarily as a function of temperature and, much less sensitively, as a function of surface gravity. The resulting estimate of R_{π} and uncertainty ΔR_{π} are independent of stellar mass and depend directly on the parallax and effective temperature. The stellar surface gravity,

$$g = \frac{GM}{R_g^2}, \tag{2}$$

provides an independent estimate of stellar radius as a function of mass. Likewise, the observed gravitational redshift V_{gr} in km s^{-1},

$$V_{gr} = 0.636\frac{M}{R_{gr}}, \tag{3}$$

provides a second relation between radius and mass in solar units. The three independent estimates of radius in equations (1) through (3) can be combined to yield a best-fitting radius (and mass) as well as the corresponding uncertainties in the mass-radius plane. This is done by minimizing the χ^2 variable,

$$\chi^2 = (\frac{R-R_\pi}{\Delta R_\pi})^2 + (\frac{R-R_g}{\Delta R_g})^2 + (\frac{R-R_{gr}}{\Delta R_{gr}})^2 \ , \tag{4}$$

In equation (4) the ΔR quantities are obtained using standard error propagation relations from the observational uncertainties, in (a) the parallax (and T_{eff} and V), (b) the surface gravity, and (c) the gravitational redshift values defined by equations (1) to (3), respectively. In calculating the uncertainty contours, we assume the $\chi2$ statistic has one degree of freedom corresponding to three independent measurements and two parameters.

Table 3: Observational Parameters for Sirius B

Sirius B	Refs.
V = 8.44 ± 0.06	1
T =24,790 ± 100 K	1
log g = 8.57 ± 0.06	1
$\pi = 0.37921'' \pm 0.00158''$	1
V_{gr} = 89 ± 16 km s^{-1}	2

1) this paper
2) Greenstein, Oke, & Shipman (1971)

In Fig. 5 we show the best-fitting masses and radii for Sirius B together with the associated 1 and 2 σ uncertainty contours. Also shown in Fig. 5 is a theoretical mass-radius relationship for a T_{eff} = 24,800 K DA white dwarf taken from the 'thick' H layer models of Wood (1995). As is evident, the best-fitting mass (0.984 ± 0.074 $M_\odot$) and radius (0.0084 ± 0.00025 $R_\odot$) for Sirius B straddles the mass-radius relation in Fig. 5. Moreover, our 1 σ contour is also clearly consistent with the range of astrometric masses independently determined by Gatewood & Gatewood (1978) for Sirius B. We have followed Shipman et al. (1997) and used the π^{-3} dependence of the mass in Kepler's Third Law to slightly revise the original Gatewood & Gatewood mass estimate of 1.053 ± 0.028 $M_\odot$ to conform to the new *Hipparcos* parallax. This new mass estimate is 1.041 ±

0.028 $M_{\odot}$. It should be noted that both our spectroscopic mass and radius for Sirius B and the Gatewood & Gatewood astrometric mass estimate are completely independent of any theoretical mass-radius relations. The spectroscopic mass-radius contours and the range of astrometric masses in Fig. 5 are mutually consistent at the 1 σ level. Combining both empirical determinations yields M = 1.034 $\pm$ 0.026 $M_{\odot}$ and R = 0.0084 $\pm$ 0.00025 $R_{\odot}$. This range of values, indicated by the heavy trapezoid in Fig. 5, is tantalizing close to the 28,000 K Wood mass-radius relation and certainly consistent with it below the 2 σ level

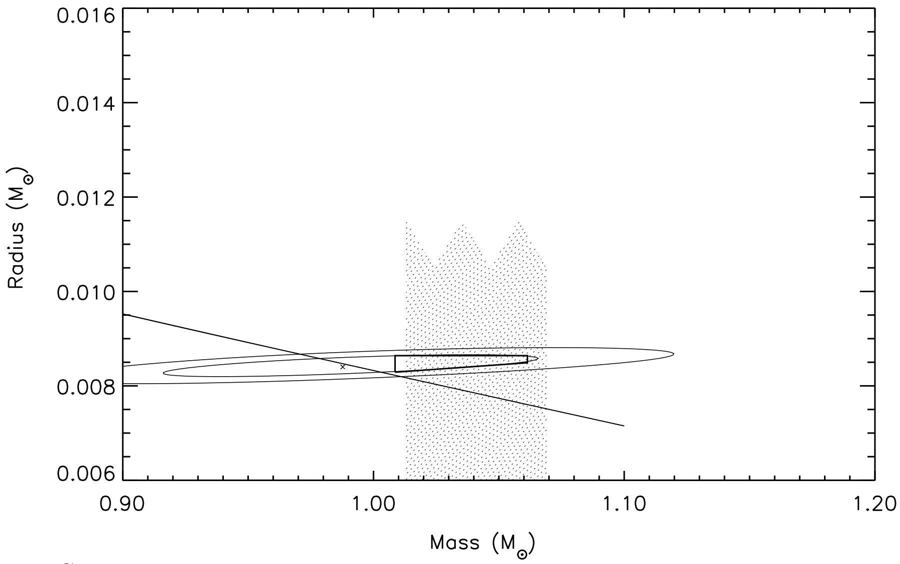

Fig. 5.— The Sirius B mass and radius in solar units with respect to the mass-radius relation for carbon-core white dwarfs. The contours are 1 σ and 2 σ χ^2 regions implied by the observed distance, temperature, surface gravity, and gravitational redshift of Sirius B. The vertical stippled region is the range of the revised astrometric mass for Sirius B from Gatewood & Gatewood (1978). The heavy trapezoid is the joint 1 σ spectroscopic and astrometric estimate of the Sirius B mass and radius.

The good agreement between the mass-radius relation and Sirius B at 1 $M_{\odot}$ helps to empirically define the high-mass end of the mass-radius relationship. It also complements very nicely the recent results of Shipman et al. (1997) who used the *Hipparcos* parallax for 40 Eri B to define the mass-radius relation at 0.5 $M_{\odot}$, near the lower mass limit for singly evolved white dwarfs. The primary difference between the Sirius B results presented here and those of Shipman et al. for 40 Eri B are two different assumptions concerning the thickness and composition of the outer non-degenerate envelope. Shipman et al. showed that in order to fit 40 Eri B, it is necessary to assume a conventional Hamada-Salpeter zero-temperature mass-radius relation. However, it can also be demonstrated that 40 Eri B is equally well fit using a 'thin' Wood model, defined by an evolved model having a layered envelope composed of 10^{-4} $M_{\odot}$ helium and zero hydrogen. For Sirius B we have used the so called 'thick' Wood models, defined by respective helium and hydrogen layers of 10^{-2} $M_{\odot}$ and 10^{-4} $M_{\odot}$, although at the mass and temperature of Sirius B, the 'thin' models have radii $\approx 0.005\ R_{\odot}$ less than the 'thick' models. Thus, taken together, these two relatively accurate results go a long way towards observational validation of the theoretical mass-radius relationships. Recently, Vauclair et al. (1997) presented new mass-radius estimates for 20 white dwarf stars obtained from *Hipparcos* parallaxes. Although the *Hipparcos* parallaxes show much improvement over ground-based work, considerable scatter with respect to the mass-radius relations remains and the authors concluded that only a general agreement with mass-radius relations can be established.

The level of consistency between the empirical mass and radius for Sirius B and the theoretical mass-radius relationships has several important implications. First, our Sirius B result, in combination with a similar determination for the white dwarf in the V 471 Tauri system (M = 0.72 $\pm$ 0.02 $M_{\odot}$, Barstow et al. 1997b) provides confidence in the theoretical mass-radius predictions for high-mass, carbon-core white dwarfs. Such predictions are widely used for the estimation of masses and radii from optically determined temperatures and gravities. Second, our results clearly imply that Sirius B does not possess an anomalously large radius as suggested by Thjell & Shipman (1986) who invoked a high rate of stellar rotation to explain their enhanced radius.

It is possible to estimate an age of $1.6\mathrm{x}10^{8}$ years for Sirius B from the models of Wood (1995). As noted by Bruhweiler et al. (1986) and others, such an age is completely inconsistent with Sirius B having been a red giant in the recent past and with the observed lack of remnant gas along the line-of-sight. Interestingly, the apparent consistency of the Sirius B mass and radius with standard thermally evolved white dwarf models may also constrain thermonuclear runaway models such as those of Bruhweiler et al. (1986).

Sirius A and B are a unique binary pair. The A0V primary is clearly one of the earliest main sequence stars in a binary system containing a white dwarf. As such, the white dwarf progenitor must have been a more massive star of an even earlier spectral type. From the empirical initial-to-final mass determinations of Koester & Reimers (1994), it can be estimated that the Sirius B progenitor had a mass of 6 to 7 $M_{\odot}$, the approximate mass of a B5 main sequence star. Theoretical models (D'Antona & Mazzitelli, 1995) yield a similar mass range of 6.5 to 7.0 $M_{\odot}$. There exists at least one DA + A star system with several apparent similarities to Sirius B: HR 8210. This A8m star was long known as a single-line spectroscopic binary with a 21.7 day orbital period. HR 8210 was suggested by Trimble & Thorn (1969) as having a compact companion. The companion was finally detected in the ROSAT EUV survey and identified as a white dwarf by Wonnacott, Kellett, & Strickland (1993). Landsman, Simon, & Bergeron (1993), who discuss the evolution of this system relative to that of Sirius B, find T_{eff} = 35,500 K and estimate a mass of $\mathrm{M}_{WD} > 1.1\ M_{\odot}$ for the white dwarf. Due to the much smaller orbital separation, they suggest that HR8210 B went through common-envelope evolution, unlike Sirius B which is assumed to be the product of single star evolution.

Further improvements in the determination of the mass and radius of Sirius B now depend on more accurate measurements of its surface gravity and gravitational redshift. Such improved values may be forthcoming in the next decade as the angular separation between Sirius A and B increases.

In summary, a significantly improved effective temperature of 24,790 $\pm$ 100 K and surface gravity of log g = 8.57 $\pm$ 0.06 are obtained for the white dwarf Sirius B. When combined the new *Hipparcos* parallax and the astrometric mass of Gatewood & Gatewood (1978), these results lead to refined estimates of the mass (M = 1.034 $\pm$ 0.026$M_{\odot}$ and radius (R = 0.0084 $\pm$0.00025$R_{\odot}$). This locates Sirius B adjacent to the theoretical mass-radius relation, at the 1 σ level, helping to empirically define the high-mass end of the white dwarf mass-radius relation. In addition, an upper limit of He/H = 1.8x10^{-5} on the photospheric content of helium in Sirius B is obtained.

JHB wishes to acknowledge support from NASA grants NAG5-2269 and NAG5-3472. MAB, AMC, and AJP acknowledge the support of PPARC, UK. The *IUE* Data Analysis Center (IUEDAC) and the National Space Science Data Center (NSSDC) are acknowledged for providing the archive *IUE* spectra presented here.

REFERENCES

Arenou, F. Lindegren, L., Froeche, M., Gomez, A. E., Turon, C., Perryman, M. A. C., & Wielen, R. 1995, AA, 305, 52

Barstow, M. A., Holberg, J. B., & Koester, D. 1995, MNRAS, 274, L31

Barstow, M. A., Dobbie, P. A., Holberg, J. B., Hubeny, I., & Lanz, T. 1997a, MNRAS, in press

Barstow, M. A., Holberg, J. B., Cruise, A. M. & Penny, A. J. 1997b, MNRAS, 290, 505

Barstow, M. A., Holberg, J. B., & Koester, D. 1994a, MNRAS, 268, L35

Barstow, M. A., Holberg, J. B., & Koester, D. 1994b, MNRAS, 270, 516

Bergeron, P., Wesemael, F., & Beauchamp, A. 1995, PASP, 107, 1047

Bergeron, P., Saffer, R. A. & Liebert, J. 1992, ApJ, 394, 225

Bergeron, P., Wesemael, F., & Beauchamp. A. 1995, PASP, 107. 1047

Bertin, P., Vidal-Madjar, A., Lallement, R. Ferlet, R., & Lemoine, M. 1995, A&A, 302, 889

Bruhweiler, F. C., Kondo, Y. 1982, ApJ, 259, 232 (BK82)

Bruhweiler, F. C., Kondo, Y., & Sion, E. M. Nature, 1986, 324, 235

Böhm-Vitense, E., Dettmann, T., & Kapranidis, S. 1979, ApJL, 232, L189 (BDK) ESA, 1977, The *Hipparcos* Catalogue, ESA SP-1000

D'Antona, F., & Mazzitelli, I. 1993, in *White Dwarfs* eds D. Koester & K. Werner, Lecture Notes in Physics,Springer, 93

Frisch, P. C. 1994, Science, 265, 1423

Gatewood, G. D., & Gatewood, C. V. 1978, ApJ, 225, 191

Gloeckler, G., Fisk, L. A., Geiss, J. 1997, Nature, 386, 374

Greenstein, J. L., Oke, J. B., & Shipman, H. L. 1971, ApJ, 169, 563

Hamada, T. & Salpeter, E. E. 1961, ApJ, 134, 683

Hardie, R. 1969 Bull. AAS, 1, 11

Holberg, J. B., Wesemael, F., & Hubeny, I. 1984, ApJ, 280, 679 (HWS)

Kidder, K., Holberg, J. B., & Wesemael, F. 1989, in *White Dwarfs* IAU Colloq. No. 114, G. Wegner ed. Springer-Verlag, p350

Koester, D. 1979, AA, 72, 376

Koester, D. 1991, in IAU Symp. 145, Evolution of Stars: The Photospheric Abundance Connection, eds. G. Micahud & A. Tutukov (Dordrecht: Kluwer), 435

Koester, D., & Reimers, D. 1996, A&A, 313, 810

Lallement, R., Bertin, P., Ferlet, R., Vidal-Madjar, A., Bertaux, J. L. 1994, A&A, 286, 898

Landsman, W., Simon, T., & Bergeron, P. 1993, PASP, 105, 841

Lindenblad, I. W. 1970, AJ, 75, 205

Paerels, F. B. S., Bleeker, J. A. M., Brinkman, A. C., & Heise, J. 1988, ApJ, 329, 849

Rakos, K. D. & Havlen, R. J. 1977, A&A, 61, 185

Renzini, A., Bragaglia, A., Ferraro, F. R., Gilmozzi, R., Ortoloni, S., Holberg, J. B., Liebert, J., Wesemael, F., & Bohlin, R. C. 1996, ApJL, 465, L23

Rumph, T., Bowyer, S. & Vennes, S. 1994, AJ, 107, 2108

Savage, B. D., & Sembach, K.R. 1996, Ann. Rev. Astron. Astrophys. 34, 279

Schmidt, H. 1996, A&A, 311, 852

Schlosser, W., & Bergmann, W. 1985, Nature, 318, 45

Shaffer, R. A., Haberi, F., Arnaud, K. A., & Tennant, A. F. 1991, ESA TM-09

Shipman, H. L., Provencal, J. L., Høg, E. & Thejll, P. 1997, ApJ, 488, L43

Sion, E. M., Greenstein, J. L., Landstreet, J. D., Liebert, J., Shipman, H. L., & Wegner, G. A. 1983, ApJ, 269, 253

Thejll, P. & Shipman, H. L. 1986, PASP, 98, 922

Trimble, V. L., & Thorne, K. S. 1969, ApJ, 156, 1013

van Altena, W. F., Truen-Liang Lee, J., Hoffleit, E. D. 1991 The General Catalogue of Trigonometric Stellar Parallaxes

Vauclair, G., Schmidt, H., Koester, D., & Allard, N. 1997, preprint

Wonnacott, D., Kellett, B. J., & Stickland, D. J. 1993, MNRAS, 262, 277

Wood, M. A. 1992, ApJ, 386, 539

Wood, M. A. 1995, in *White Dwarfs* eds D. Koester & K. Werner, Lecture Notes in Physics, Springer, 41

Wood, B. E., & Linsky, J. L. 1997, ApJL, 474, L39